TRIPERIODIC STRUCTURE*

B. Epsztein - Tran Duc Tien
C. S. F.
Domaine de Corbeville
Orsay (91), France

Summary

A number of alternating periodic structures have been described which operate with a $\pi/2$ phase shift between adjacent cavities, simulating a π mode configuration while alternate cavities remain empty. In this paper, it is shown that similar properties can be obtained with a structure operating with a $2\pi/3$ phase shift. The basic cell, made of three cavities, is one wavelength long. If correct terminating conditions are satisfied, a standing wave pattern can be set up which simulates the π mode field in two cavities, the third being empty.

Two cases are being considered:

1) An iris structure where the empty cavities have a reduced length with respect to the others. Calculations and measurements show that the impedance is improved with respect to the corresponding $\pi/2$ structure, due to the fact that there is only one empty cell per wavelength instead of two, while other electrical properties remain unchanged.

2) A drift tube structure is also investigated. The coupling cavities are so designed as to prevent their direct excitation by the beam.

Introduction

Biperiodic structures have been studied several years ago at Brookhaven National Laboratory,[1,2] at Los Alamos Scientific Laboratory[3] and at CERN.[4,5]

For two years, structure studies have been carried out in this direction at our Laboratory. It appears that, in a certain form, the triperiodic structure could present some advantages. By "biperiodic" or "triperiodic" we mean structures, the period of which is made of two or three cavities, or more generally speaking, of two or three resonant systems (cavities or stems...). Figure 1 illustrates schematically the operation of the bi and triperiodic structures. Forward and backward waves, represented respectively by solid and dashed arrows, combine themselves in the 2π mode to cancel the field in the coupling cavities, as can be shown in the vector diagrams. One can see, for instance, that in the triperiodic operation case, the solid and dashed vectors 1, 2 and 3 representing forward and backward wave fields in the corresponding cavities, add together in cavities 2 and 3 but, on the other hand, cancel in cavity 1. The fact that one out of two coupling cavities could be eliminated, involving a gain of space, and simplifying, in certain cases, the design, makes the triperiodic structure interesting.

This paper presents briefly the theoretical results, based on lumped circuit models, of the dispersive properties of some kinds of structures, and experimental work on three typical structures.

Dispersive Properties of Lumped Circuit Models

The two models presented in Fig. 2 have been used, corresponding to the capacitive coupling case, and to the inductive coupling case. In the first model, the successive cavities, represented by the impedances Z_1 and Z_2, are loaded in parallel by the impedances Z' and Z''. The T-cell, in dashed line, represents the direct coupling between non-adjacent cavities. In the second model, the coupling is performed by mutual inductances: M, m and m' representing the coefficients of mutual inductance, respectively, between two adjacent accelerating cavities, between one accelerating cavity and the coupling one and finally between two non-adjacent accelerating cavities.

The studies of the dispersion curve (β,ω) may be performed by examining the trace of the transfer matrix of the period, which, in the case of passive circuits, contains a real part $F(\omega)$, even in respect to ω, and an odd imaginary part $G(\omega)$. In a lossless structure, $G(\omega)$ vanishes, and from $F(\omega)$ one deduces the passbands according to:

$$[\tfrac{1}{2}\ \text{Trace}\ M] \equiv [F(\omega)] \equiv [\cos\beta(\omega)] \leq 1 \qquad (1)$$

Thence the group velocity:

$$\frac{\partial\omega}{\partial\beta} = \pm \frac{\sqrt{1 - F^2(\omega)}}{\frac{\partial F}{\partial\omega}} \qquad (2)$$

So, when $\partial F/\partial\omega \neq 0$, $\partial\beta/\partial\omega$ drops to zero at the zero and k modes for which $|F(\omega)| = 1$. On

*This work is supported in part by the Département de Physique Nucléaire, Institut de Recherches Nucléaires, Strasbourg-Cronenbourg.

the other hand, when $\partial F/\partial\omega = 0$, the group velocity becomes finite and can be written as:

$$\frac{\partial\omega}{\partial\beta} = \pm\sqrt{\frac{-F(\omega_{0,\pi})}{\left(\frac{\partial^2 F}{\partial\omega^2}\right)_{\omega_{0,k\pi}}}} \qquad (3)$$

Hence, according to the form of $F(\omega)$ in the neighborhood of ± 1, one deduces the behavior of the dispersion curve in the neighborhood of splittings.

For a lossless biperiodic structure, and when coupling between non-adjacent cavities can be neglected, the dispersion function can be written as:

$$F_{2C}(\omega) = \qquad (4)$$

$$-1 + \tfrac{1}{2}C'L_1L_2\left(\omega^2_{1\pi/2} - \omega^2\right)\left(\omega^2_{2\pi/2} - \omega^2\right)$$

in the capacitive coupling case, and as:

$$F_{2I}(\omega) =$$

$$-1 + \frac{2}{K^2}\left(1 - \frac{\omega^2_{1\pi/2}}{\omega^2}\right)\left(1 - \frac{\omega^2_{2\pi/2}}{\omega^2}\right) \qquad (5)$$

with $K^2 = 4M^2/L_1L_2$, in the inductive coupling case, where $\omega_{1\pi/2}$ and $\omega_{2\pi/2}$ are defined as the pulsations of $\pi/2$ mode of structures made of cavities of the same kind. These pulsations can be excited by modifying the boundary conditions. It should be noted that (4) and (5) are classical and have been obtained by other methods.

For the lossless triperiodic structure, one obtains:

$$F_{3C}(\omega) =$$

$$-1 + \left[-\frac{L_1C'}{2}\left(\omega^2 - \omega^2_{01}\right) - L_2C'\left(\omega^2 - \omega^2_{02}\right)\right.$$

$$\left. + \frac{L_1L_2C'^2}{2}\left(\omega^2 - \omega^2_{01}\right)\left(\omega^2 - \omega^2_{02}\right)\right]$$

$$\times\left[2 + \frac{C''}{C'} - C''L_2\left(\omega^2 - \omega^2_{02}\right)\right] \qquad (6)$$

in the capacitive coupling case, and:

$$F_{3I}(\omega) = \frac{4}{KK'^2}\left(1 - \frac{\omega^2_{02}}{\omega^2}\right)\left(1 - \lambda\frac{\omega^2_{02}}{\omega^2}\right)$$

$$- \frac{2}{K}\left(1 - \frac{\omega^2_{02}}{\omega^2}\right) - \frac{K}{K'^2}\left(1 - \lambda\frac{\omega^2_{02}}{\omega^2}\right) \qquad (7)$$

in the inductive coupling case, with:

$$K = \frac{2M}{L}\ ,\ K' = \frac{2M}{\sqrt{LL'}}\ ,\ \lambda = \frac{\omega^2_{01}}{\omega^2_{02}}$$

where ω_{01} and ω_{02} are successively the resonance pulsations of coupling and accelerating cavities. Figure 3 shows the variations of the dispersion function of a triperiodic structure. Generally, one observes three distinct passbands. However, from relations (6) and (7) one can deduce the conditions that parameters must fulfill so that one of the splittings vanishes particularly at the 2π mode. It comes out that, to realize the continuity of the dispersion curve, several methods are possible. For instance, coupling can be kept constant between different kinds of cavities, then one must have:

$$\omega_{1\ 2\pi/3} = \omega_{2\ 2\pi/3} \qquad (8)$$

where $\omega_{1\ 2\pi/3}$ and $\omega_{2\ 2\pi/3}$ are defined as the 2π mode pulsations of structures built with each kind of cavity. On the contrary, the frequencies can be kept constant, then coupling coefficients must be in a correct ratio.[6,7] These two different tuning methods leave the phase shift of the whole period unchanged, but modify the one between elementary cells. The condition (8) corresponds for instance to the case of identical phase shift between successive cavities, i.e., $2\pi/3$. As long as the adjacent accelerating cavities are the same, one can see, from a simple vector diagram like that on Fig. 1, that, in any case, the operation should be altered.

If the length of the coupling cavities grows small relative to the coupling hole diameter and also if these holes are facing each other, the fringing field introduces between non-adjacent accelerating cavities a direct coupling which must be taken in account in the dispersion function. From the models of Fig. 3, the new trace (M') can be calculated. For instance, in the inductive coupling case, one has:

$$\text{Trace } (M') = \frac{1}{1 - \frac{jm'\omega Z_1}{m^2\omega^2}} \qquad (9)$$

$$\left[\frac{1}{2}\text{ Trace }[M] - \frac{m'}{2M}\left(2 - \frac{jm'\omega}{m^2\omega^2}Z_1\right)\right]$$

The supplementary terms explain the deformation of the dispersion curves.

Studies including losses have also been carried out. It comes out that losses do not affect the dispersion curve in a sensible manner, except in the neighborhood of the 0 and 3π mode. One finds an infinite branch at the 0 mode, and at the 3π mode, the dispersion curve drops to $\omega = 0$ with a slope equal to $- QQ'/2Q' + Q$, Q and Q′ corresponding respectively to accelerating and coupling cavities. However, one could make sure that the losses should not introduce dangerous phase shift. Dispersion functions are given as:

$$F(u) = \frac{4}{K^3}\frac{1}{u^3}\left(u - \frac{1}{u}\right)\left[\left(u - \frac{1}{u}\right)^2 - \frac{1}{Q}\left(\frac{1}{Q'} + \frac{2}{Q}\right)\right] + \frac{3}{Ku}\left(u - \frac{1}{u}\right) \qquad (10\text{-}1)$$

$$G(u) = \frac{4}{K^3u^3}\left[\frac{1}{Q'Q^2} - \left(\frac{1}{Q'} + \frac{2}{Q}\right)\left(u - \frac{1}{u}\right)^2\right] + \left(\frac{2}{Q} + \frac{1}{Q'}\right)\frac{1}{Ku} \qquad (10\text{-}2)$$

with $u = \omega/\omega_0$. G(u) can be then put in a more convenient form:

$$\left(\frac{1}{Q'} + \frac{2}{Q}\right)\left(\frac{K^2}{4} - 1\right)u^4 + \left[\frac{1}{Q'Q^2} + 2\left(\frac{1}{Q'} + \frac{2}{Q}\right)\right]u^2 - \left(\frac{1}{Q'} + \frac{2}{Q}\right) = \frac{K^3}{4}u^5 \sinh\alpha \sin\beta \qquad (11)$$

which admits, provided:

$$\frac{1}{Q'Q^2} \ll 2\left(\frac{1}{Q'} + \frac{2}{Q}\right) \qquad (12)$$

as it is always the case, the following solutions:

$$\beta = 2\pi$$
$$u^2 = \left(1 \pm \frac{K}{2}\right)^{-1} \qquad (13)$$

that can be easily verified as the lossless solutions.

By the way, the phase shift due to losses can be calculated, and one obtains:

$$\sin\Delta\beta = \frac{\frac{K}{\sqrt{2}}\left(1 + \frac{K}{2}\right)}{Q\sqrt{\frac{Q}{Q'}}\left(1 + \frac{2Q'}{Q}\right)^{3/2}}$$

This does not in any way exceed 10^{-6}.

Thus, in the triperiodic operation, losses do not affect the phase shift of the whole period. Of course, phase shifts between elementary cells would change but would cancel after a whole period.

Experimental Results

Studies are carried out for three types of structures shown in Fig. 4, in both biperiodic and triperiodic operations. Type I is derived directly from a travelling wave electron structure; its coupling holes are rather large for a good shunt impedance in standing wave operation. Type II is somewhat closer to a proton structure; transit time is lowered there by drift tubes. Coupling is achieved by four circular holes. In the type III, the coupling cavities are designed so that the beam should not be directly coupled to them. Pictures can be seen in Figs. 5, 6 and 7.

Figure 8 shows the dispersion curve of a biperiodic structure of type I. One can see that the direct coupling between non-adjacent cavities has correctly been represented by the model used.

Figure 9 shows the effect of the iris aperture on the splitting. The continuity of the dispersion curve can be verified by changing the boundary conditions so that the two frequencies of the splitting could be excited. Indeed, one of these frequencies could be obtained by cutting the structure at the middle of the coupling cavity. To obtain the other one, the structure must be ended by two identical cavities adequately tuned, as shown in Fig. 1, so that the forward waves, starting from the last coupling cavity, should undergo a phase shift of π when they come back, after being reflected on the shorting plates. It comes out that this tuning is rapidly convergent, and zero field is easily settled in coupling cavities after some manipulations.

Figure 10 shows dispersion curves calculated and measured on the triperiodic structure of type I.

Figures 11 and 12 show curves obtained on structures of type II, in biperiodic and triperiodic operations.

Figures 13 and 14 show the same curves of type III.

One observes good agreement between calculated and measured points. The coupling parameters and frequencies shown are theoretical ones.

The following table gives experimental results on the shunt impedance and Q value of different structures. The Q values indicated, correspond to an infinite structure. They are obtained from measurements on different structure lengths.

Measurements on type I allow a comparison between the bi and triperiodic operations. The efficient gain observed in the latter consists chiefly in the Q value. As for Z/Q, the transit time works favorably in the biperiodic operation, when the coupling cavity lengths increase as can be seen in the 2nd and 3rd cases. In the 4th and 5th cases, where transit times are the same, the slightly lower Z/Q value of the triperiodic structure is due to the central coupling aperture which has been enlarged in order to realize continuity of the dispersion curve. The low shunt impedances obtained are due to the large coupling holes (28.2 mm of diameter). Another biperiodic structure has been built with smaller hole diameter (22 mm), and recent measurements give a Q value of 14,000 and a Z value of 42.2 MΩ/m at $\beta = 1$, and F = 2,840 MHz, with 2.6% of bandwidth. An analogous triperiodic structure will be measured soon.

Results obtained from type II structure are encouraging.

As for type III, the Q value indicated is but a lower limit value, contacts being indeed very bad. An 18 cell tank will be brazed soon.

Deflecting Modes

Deflecting TM_{11} mode investigations are carried out for each kind of structure, in both bi and triperiodic operations. Two or three passbands can be observed according to whether the type of structure is bi or triperiodic. Let us consider the first case, the phenomena being indeed the same for the last case.

As the resonant frequencies of coupling and accelerating cavities are separated at the TM_{11} mode, due either to the effects of coupling holes, which are not the same in each kind of cavity or due to the difference of their form, one can observe one very narrow passband belonging to the set of coupling cavities, slightly coupled by fringing field across accelerating cavities, and one relatively larger one belonging to the set of accelerating cavities, well coupled across the coupling cavities. The splitting between these bands is not very large in type I (3.2%) and consequently the two passbands are important (0.28% and 1.75%).

On the other hand, these two passbands are highly separated in type II or III. Furthermore, they could be greatly reduced if the coupling holes did not face each other. In the type III case, for instance, one observes a splitting of 33% with ~ 0% for the lower band and 2.5% for the upper one, which drops to 0.44%, when holes are no longer facing each other. It seems to be an interesting result, for this could be a simple method of eliminating the danger of the deflecting mode, by preventing it from propagating along the tank: each cavity acts now indeed like an isolated one.

References

1. T. Nishikawa, S. Giordano, and D. Carter Brookhaven National Laboratory Accelerator Department Internal Report AADD 88, August 1965.

2. S. Giordano and J. P. Hannwacker, Proceedings of the 1966 Linear Accelerator Conference, October 1966, p. 88, Los Alamos.

3. B. C. Knapp, E. A. Knapp, G. P. Lucas, and J. M. Potter, IEEE Trans. Nucl. Sci. NS-12, No. 3, 159 (1965).

4. A. Carne, G. Dome, International Conference on High Energy Accelerators, Frascati, September 1965.

5. G. Dome, I. White, Proceedings of the 6th International Conference on High Energy Accelerators at Cambridge, September 11 - 15, 1967, p. A.19.

6. D. T. Tran, Institut de Recherches Nucléaires de Strasbourg-Cronenbourg, Rapport de fin d'études WR 1678, December 1966.

7. B. Epsztein, D. T. Tran, Institut de Recherches Nucléaires de Strasbourg-Cronenbourg, Rapport de fin d'études DAC 4752, December 1967.

Table. Experimental results of shunt impedance and Q value of different structures.

TYPE	h_1 mm	h_2 mm	$\beta = \frac{v}{c}$	F_{GHz}	Mode	Q	$(\frac{Z}{Q})_{eff}$ Ω/m	T	Z_{eff} MΩ/m
I	13,7	30,3	0,93	2,78	BI	11.000			
	13,7	30,3	0,787	2,83	TRI	11.300	2000	0,815	22,66
	13,7	23,5	0,8	2,795	BI	9.850	1930	0,86	19
	6,7	30,3	0,718	2,83	TRI	11.500	1770	0,78	20,4
	6,7	25,3	0,71	2,796	BI	8.650	1880	0,785	16
II			0,65	2,618	TRI	13.000	5290	0,848	68,77
III			0,6	0,943	TRI	>11.000	2340	0,888	>26

h_1 = Lenght of the coupling cavities

h_2 = ——— accelerating cavities

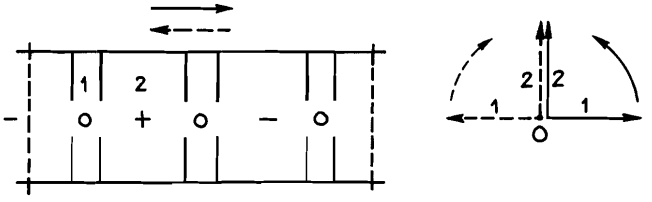

BIPERIODIC SYSTEM

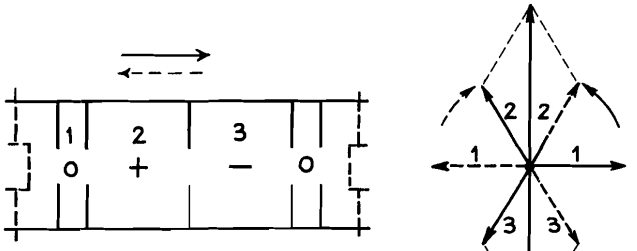

TRIPERIODIC SYSTEM

Figure 1 - Schematic representation of bi and triperiodic structures. The forward and backward waves are represented by solid and dashed arrows respectively.

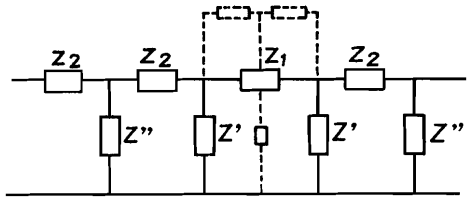

(CAPACITIVE COUPLING)

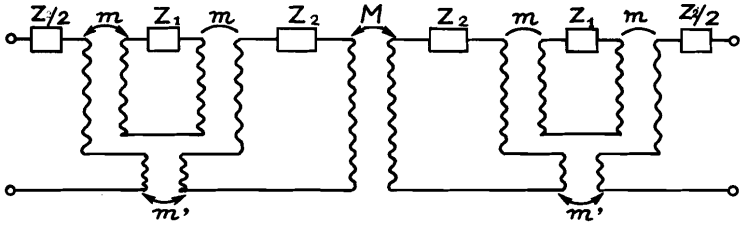

(INDUCTIVE COUPLING)

Figure 2 - Equivalent circuits used to represent the triperiodic structure.

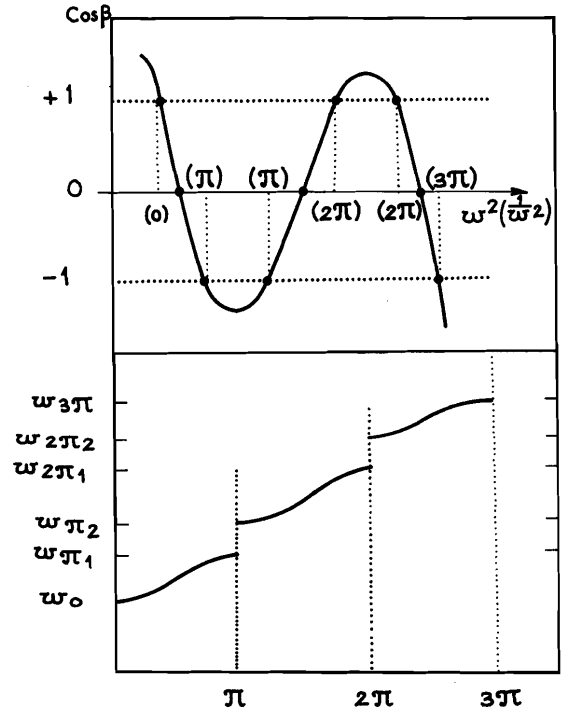

Figure 3 - Dispersion curve for the triperiodic structure.

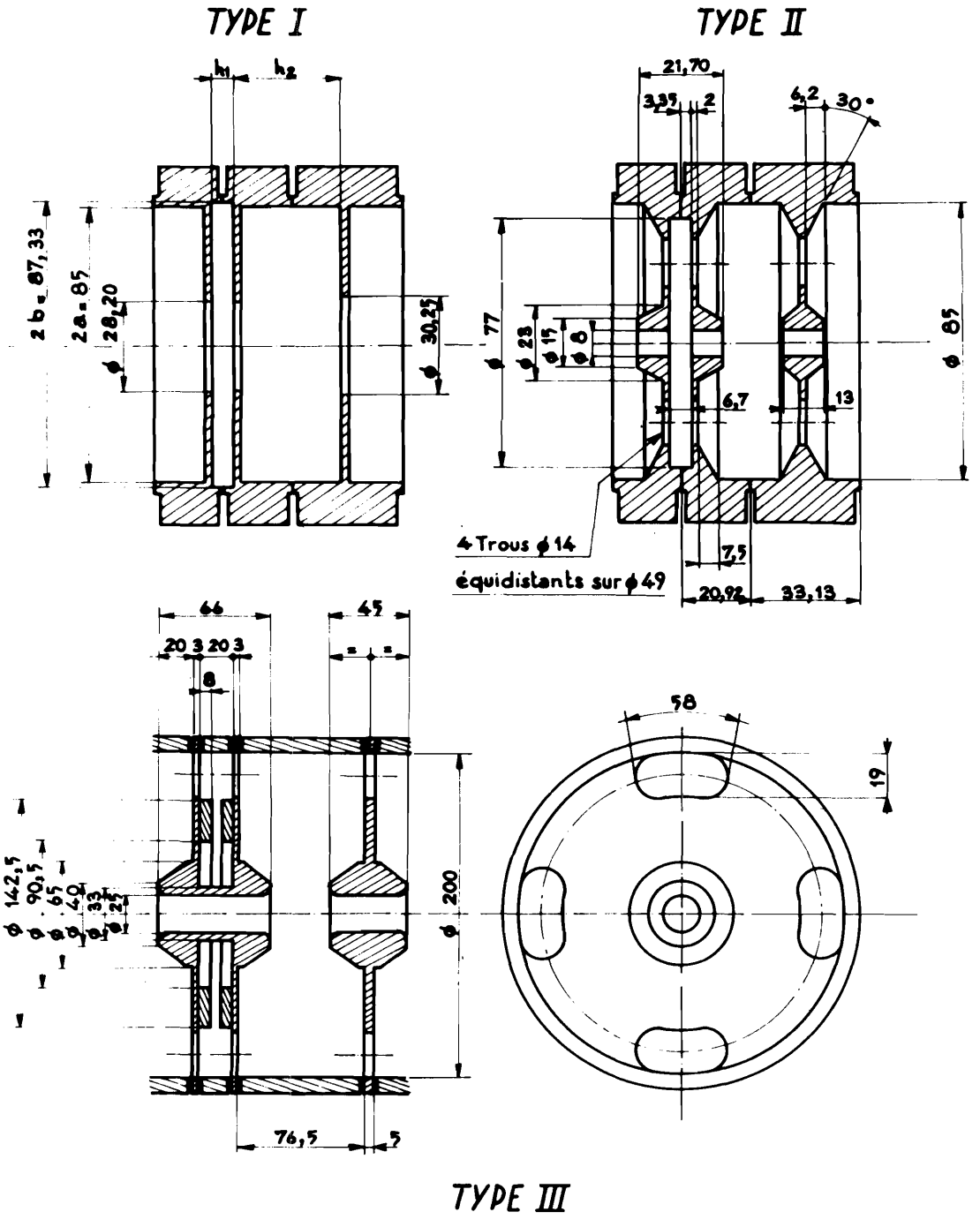

Figure 4 - Three types of structures for which studies have been carried out.

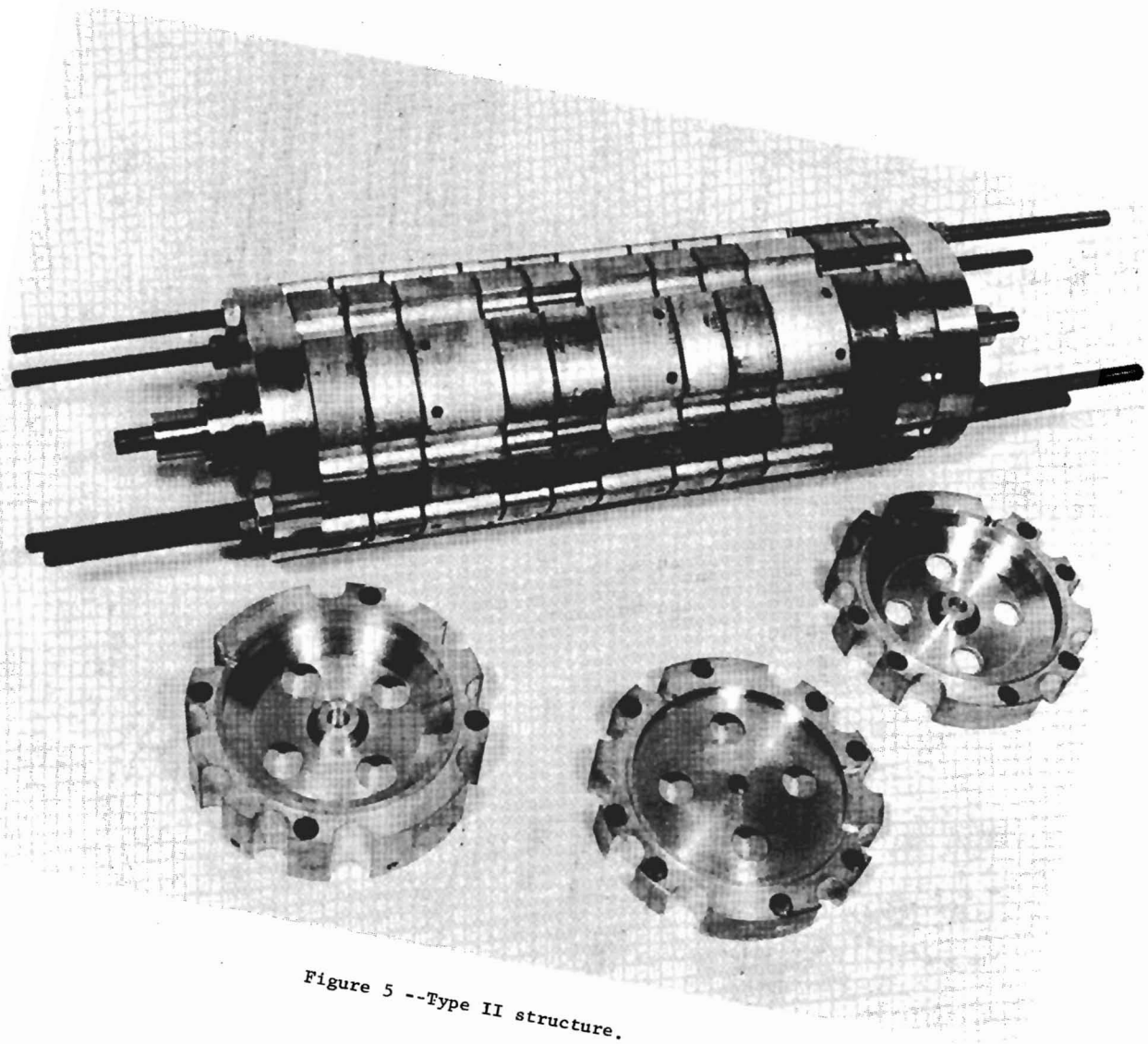

Figure 5 --Type II structure.

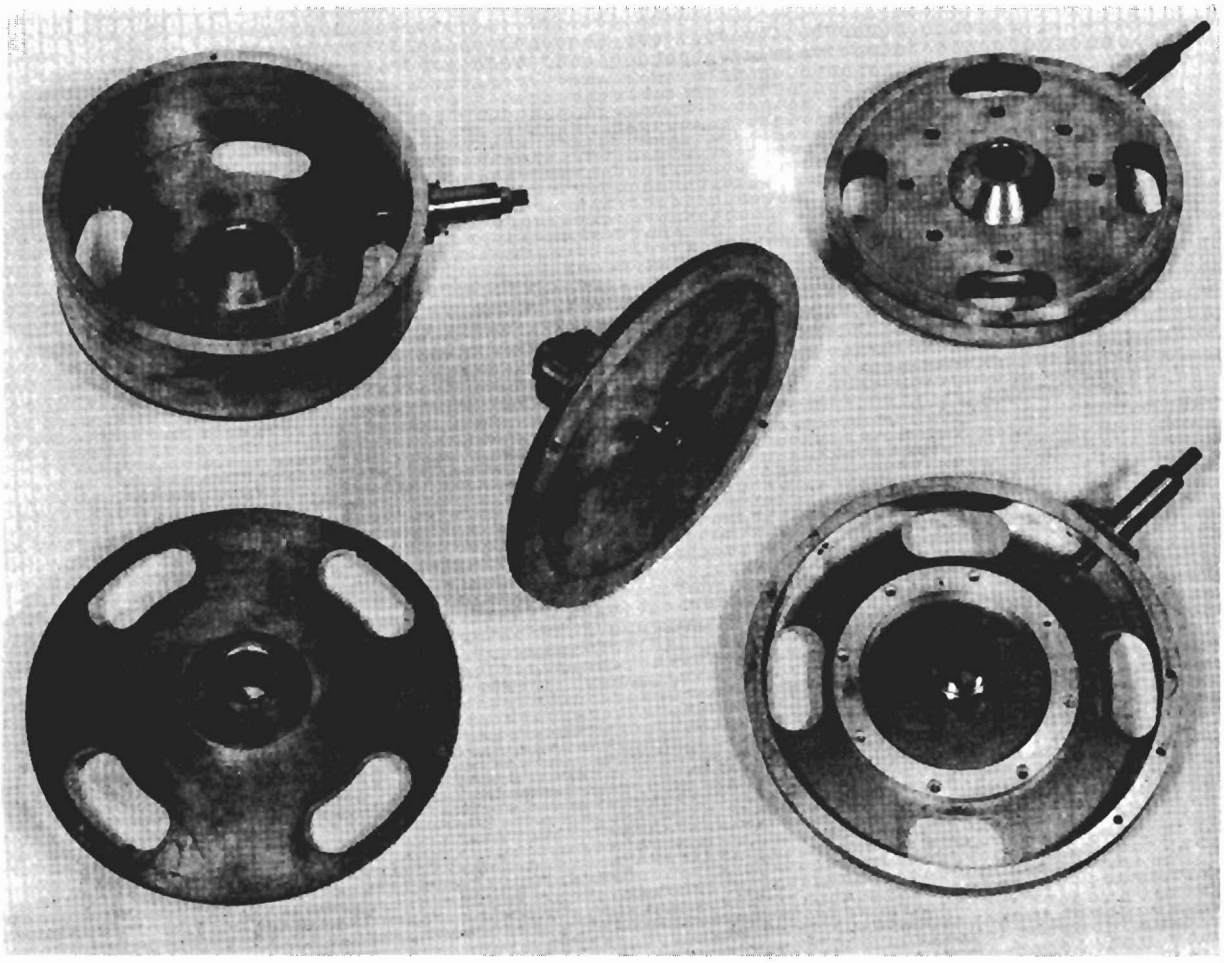

Figure 6 - Type III structure.

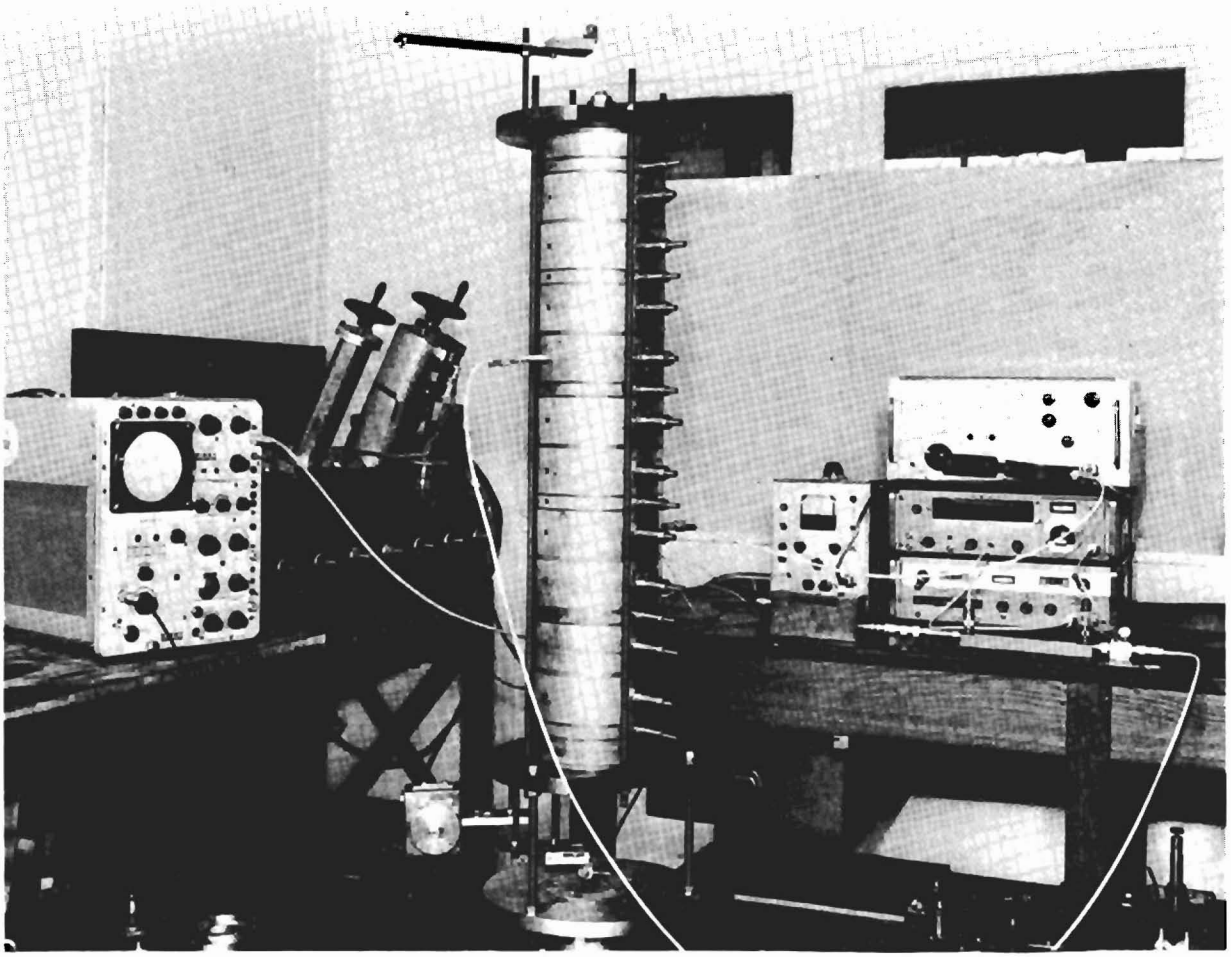

Figure 7 - Assembled cavity.

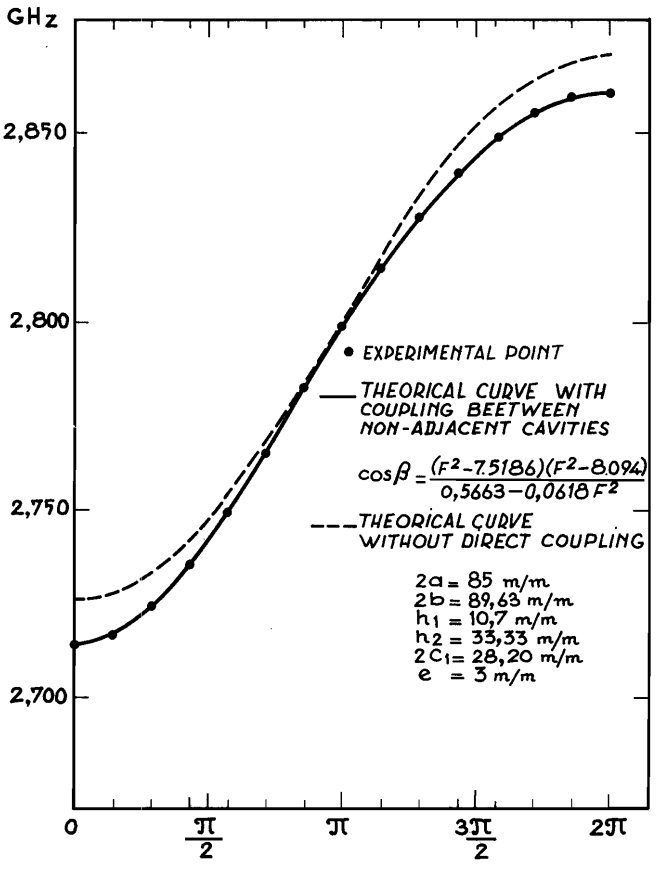

Figure 8 - Dispersion curve of a biperiodic structure of type I.

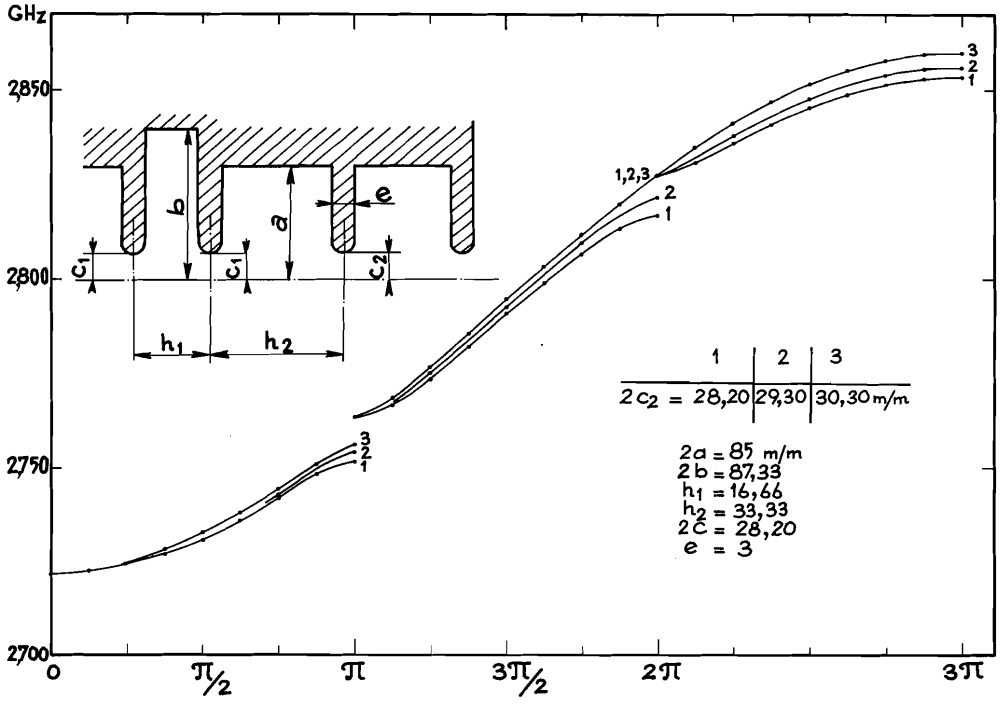

Figure 9 - Effect of iris aperture on splitting for the type I triperiodic structure.

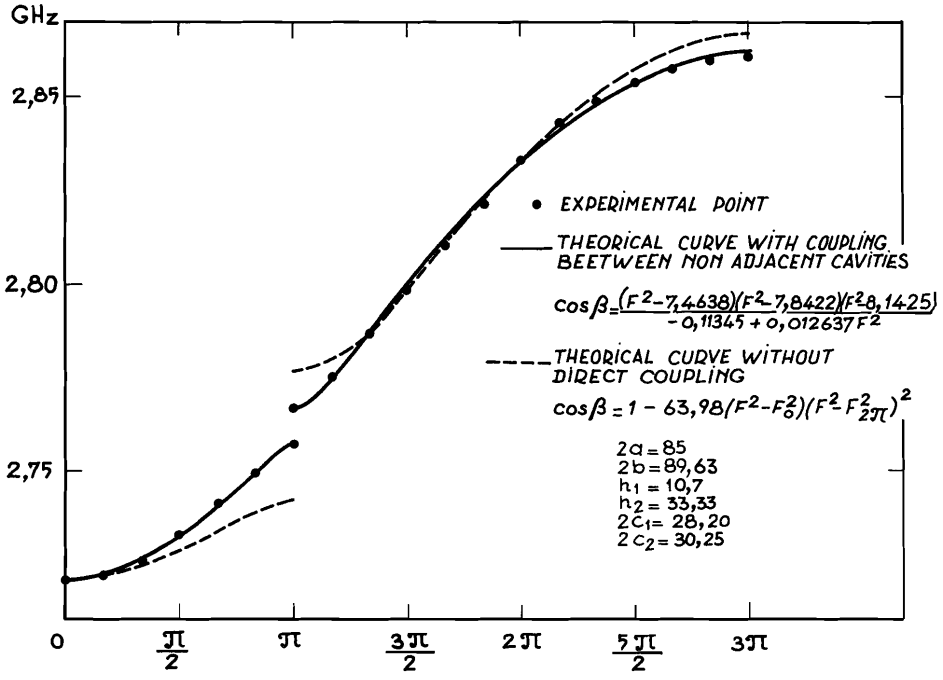

Figure 10- Calculated and measured dispersion curve for the triperiodic structure of type I.

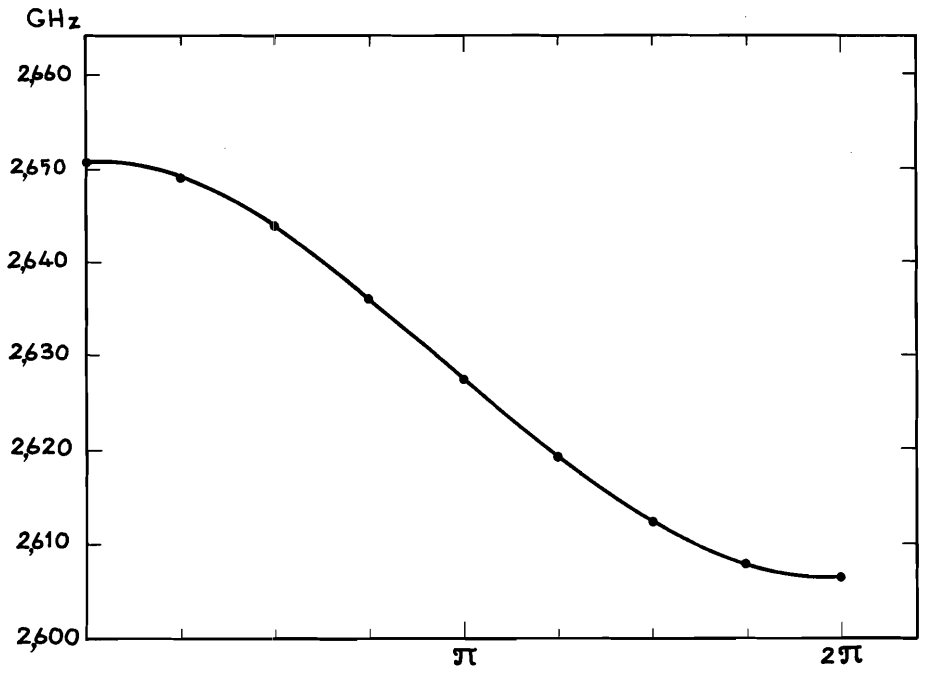

Figure 11- Dispersion curve for the biperiodic structure of type II.

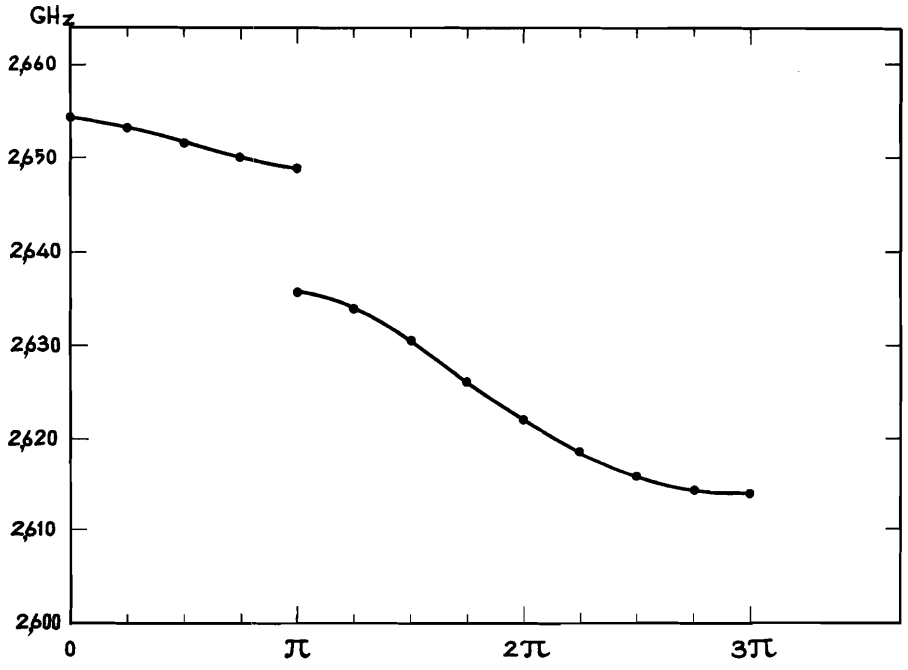

Figure 12- Dispersion curve for the triperiodic structure of type II.

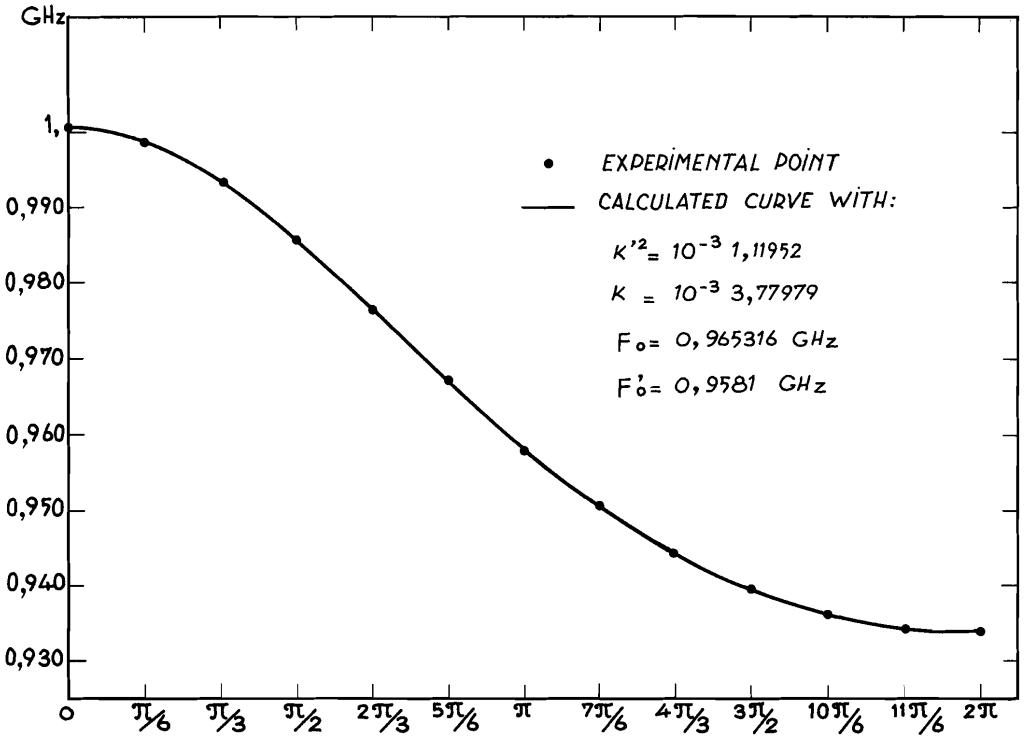

Figure 13- Dispersion curve for the biperiodic structure of type III.

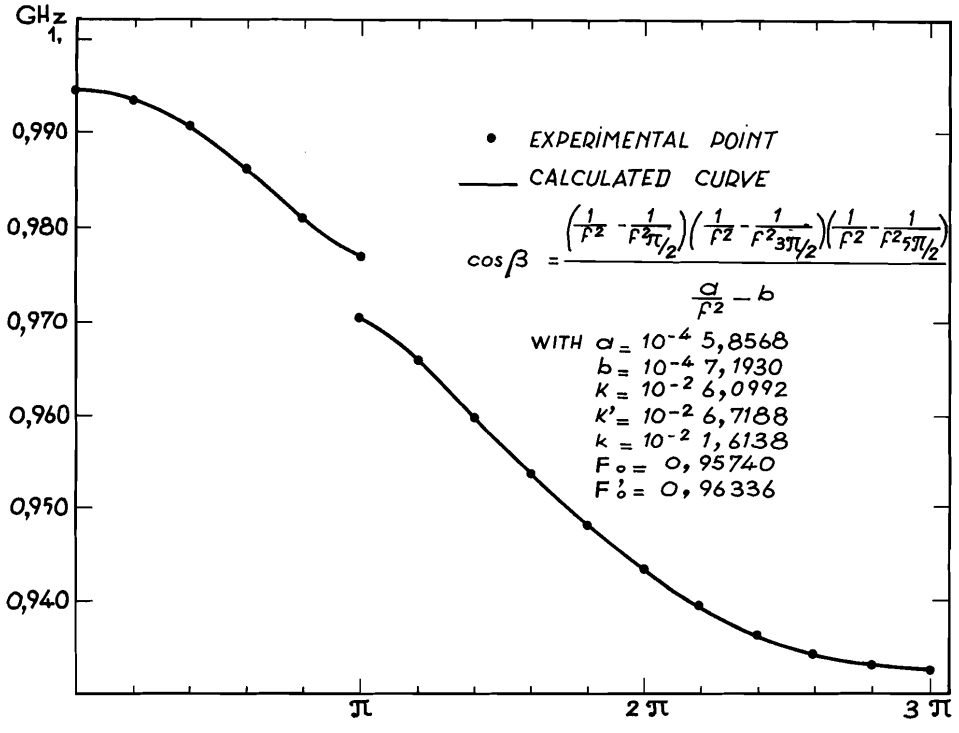

Figure 14- Dispersion curve for the triperiodic structure of type III.